

# Angular momentum of optical vortex arrays

**Johannes Courtial**

*Department of Physics & Astronomy, University of Glasgow, Glasgow, G12 8QQ, UK*

[j.courtial@physics.gla.ac.uk](mailto:j.courtial@physics.gla.ac.uk)

**Roberta Zambrini**

*Department of Physics, University of Strathclyde, 107 Rottenrow, Glasgow, G4 0NG, UK*

**Mark R Dennis**

*School of Mathematics, University of Southampton, Highfield, Southampton, SO17 1BJ, UK*

**Mikhail Vasnetsov**

*National Academy of Sciences of Ukraine, Kiev, Ukraine*

**Abstract:** Guided by the aim to construct light fields with spin-like orbital angular momentum (OAM), that is light fields with a uniform and intrinsic OAM density, we investigate the OAM of strictly periodic arrays of optical vortices with rectangular symmetry. We find that the OAM per unit cell depends on the choice of unit cell and can even change sign when the unit cell is translated. This is the case even if the OAM in each unit cell is intrinsic, that is independent of the choice of measurement axis. We show that spin-like OAM can be found only if the OAM per unit cell vanishes. Our results are applicable to the  $z$  component of the angular momentum of any  $x$ - and  $y$ -periodic momentum distribution in the  $xy$  plane, and can also be applied to other periodic light beams and arrays of rotating solids or liquids.

© 2006 Optical Society of America

**OCIS codes:** (999.9999) Optical angular momentum; (999.9999) Optical vortices, mechanics.

---

## References and links

1. J. H. Poynting, "The Wave Motion of a Revolving Shaft, and a Suggestion as to the Angular Momentum in a Beam of Circularly Polarised Light," *Proc. R. Soc. London, Ser. A* **82**, 560–567 (1909).
2. L. Allen, M. W. Beijersbergen, R. J. C. Spreeuw, and J. P. Woerdman, "Orbital angular momentum of light and the transformation of Laguerre-Gaussian modes," *Phys. Rev. A* **45**, 8185–8189 (1992).
3. A. T. O'Neil, I. MacVicar, L. Allen, and M. J. Padgett, "Intrinsic and extrinsic nature of the orbital angular momentum of a light beam," *Phys. Rev. Lett.* **88**, 53,601 (2002).
4. M. Berry, "Paraxial beams of spinning light," in *Singular Optics*, M. S. Soskin, ed., vol. 3487 of *Proc. SPIE*, pp. 1–5 (SPIE - the International Society for Optical Engineering, Bellingham, Wash., USA, 1998).
5. S. M. Barnett, "Optical angular-momentum flux," *J. Opt. B: Quantum Semiclass. Opt.* **4**, S7–S16 (2002).
6. I. Dana and I. Freund, "Vortex-lattice wave fields," *Opt. Commun.* **136**, 93–113 (1997).
7. R. M. Jenkins, J. Banerji, and A. R. Davies, "The generation of optical vortices and shape preserving vortex arrays in hollow multimode waveguides," *J. Opt. A: Pure Appl. Opt.* **3**, 527–532 (2001).
8. A. Dreischuh, S. Chervenkov, D. Neshev, G. G. Paulus, and H. Walther, "Generation of lattice structures of optical vortices," *J. Opt. Soc. Am. B* **19**, 550–556 (2002).
9. F. S. Roux, "Optical vortex density limitation," *Opt. Commun.* **223**, 31–37 (2003).
10. R. Zambrini, L. C. Thomson, S. M. Barnett, and M. Padgett, "Momentum paradox in a vortex core," *J. Mod. Opt.* **52**, 1135–1144 (2005).

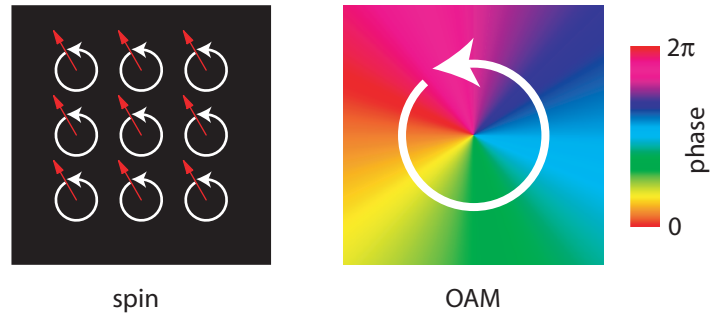


Fig. 1. Rotation of spin (left) and orbital angular momentum (OAM, right) states. The left plot shows the local electric field vector (red arrows) in a number of positions in a circularly polarised plane wave. The right plot shows a colour representation of the local phase (red  $\rightarrow$  green  $\rightarrow$  blue  $\rightarrow$  red represents a full  $2\pi$  phase cycle) of an  $m = 1$  optical vortex. Whereas the spin state rotates around every point, the OAM state rotates around the beam axis. The rotation is indicated here by white arrows; it can clearly be seen in the movies of the time evolution over one optical period of spin (48 KB) and OAM (204 KB), which are contained in the additional multimedia material.

11. K. Ladavac and D. G. Grier, "Microoptomechanical pumps assembled and driven by holographic optical vortex arrays," *Optics Express* **12**, 1144–1149 (2004). URL <http://www.opticsexpress.org/abstract.cfm?URI=OPEX-12-6-1144>.
12. M. R. Dennis and J. H. Hannay, "Saddle points in the chaotic analytic function and Ginibre characteristic polynomial," *J. Phys. A: Math. Gen.* **36**, 3379–3383 (2003).
13. J. R. Abo-Shaeer, C. Raman, J. M. Vogels, and W. Ketterle, "Observation of Vortex Lattices in Bose-Einstein Condensates," *Science* **292**, 476–479 (2001).
14. R. Donnelly, *Quantized Vortices in Helium II* (Cambridge University Press, Cambridge, 1991).
15. P. G. Saffman, *Vortex Dynamics* (Cambridge University Press, Cambridge, England, 1992).
16. J. Sommeria, "Experimental study of the two-dimensional inverse energy cascade in a square box," *J. Fluid Mech.* **170**, 139–168 (1986).
17. D. L. Boiko, G. Guerrero, and E. Kapon, "Polarization Bloch waves in photonic crystals based on vertical cavity surface emitting laser arrays," *Opt. Express* **12**, 2597–2602 (2005). URL <http://www.opticsexpress.org/abstract.cfm?URI=OPEX-12-12-2597>.
18. K. Paturski, "The self-imaging phenomenon and its applications," *Progr. Opt.* **XXVII**, 3–108 (1989).
19. L. Mandel and E. Wolf, *Optical Coherence and Quantum Optics* (Cambridge University Press, Cambridge, 1995).
20. J. Courtial, K. Dholakia, L. Allen, and M. J. Padgett, "Gaussian beams with very high orbital angular momentum," *Opt. Commun.* **144**, 210–213 (1997).

## 1. Introduction

At the heart of angular momentum lies rotation: angular momentum is conserved due to the isotropy of space (i.e. invariance under rotations); the conjugate variable in the quantum-mechanical uncertainty pair to angular momentum is rotation angle; and, of course, rotating objects have angular momentum. It is therefore unsurprising that rotating light beams have angular momentum.

Light beams can rotate in more than one way, and these different types of rotation correspond to different types of angular momentum (Fig. 1). In circularly polarised light beams the electric field vector at every point rotates uniformly [1]; these correspond to quantum-mechanical spin states. In other light beams the phase structure rotates uniformly about the beam axis, which is marked by a phase singularity (optical vortex line); these correspond to orbital angular momentum (OAM) states [2]. A light beam in which both the phase structure *and* the electric field vectors at every point rotate uniformly corresponds to a total angular momentum state; we do

not consider such states here.

This rotation of the light itself is reflected in the mechanical effects the light's spin and OAM have when transferred to a microscopic object: spin causes spinning about the object's centre of mass while OAM causes orbiting about the (local) center of light rotation, which in the case of OAM states is the beam centre [3]. Such a distinction between the spin and OAM of a light beam is also meaningful mathematically [4, 5].

The OAM in a uniformly polarized, monochromatic, paraxial light beam is due to the transverse linear momentum density,  $\mathbf{p}_\perp$ , which is related to the polarization-independent complex field,  $\psi$ , through the equation

$$\mathbf{p}_\perp(\mathbf{r}) = \text{Im}(\psi^* \nabla_\perp \psi), \quad (1)$$

where  $\mathbf{p}_\perp = (p_x, p_y)$ ,  $\mathbf{r} = (x, y)$  and  $\nabla_\perp = (\partial/\partial x, \partial/\partial y)$ . This corresponds to an OAM density in the  $z$  direction of

$$\omega(\mathbf{r}) = (\mathbf{r} \times \mathbf{p}_\perp(\mathbf{r}))_z \equiv xp_y - yp_x. \quad (2)$$

(We are interested in the angular momentum in the direction of light propagation,  $z$ . From now on we will simply refer to (orbital) angular momentum, without explicit mention of the  $z$  direction.) An area  $A$  then has OAM

$$\Omega_A = \int_A \omega(\mathbf{r}) \, dx \, dy \quad (3)$$

and a (semi-classical) OAM per photon in units of  $\hbar$  [2] – the ratio of the OAM and energy contained in  $A$  – of

$$l = \Omega_A / \left( \int_A |\psi|^2 \, dx \, dy \right). \quad (4)$$

Whereas OAM effects happen relative to the center of light rotation, spin effects happen locally. It is therefore not surprising that spin angular momentum is intrinsic – its value does not depend on the position of the point relative to which the spin is measured. Perhaps surprisingly, OAM can also be intrinsic [4]: in spite of the fact that light beams in OAM states rotate around one particular axis, the value of one component of the OAM vector, namely the component in the direction of the (linear) momentum of the beam, is independent of the choice of origin. We choose to align our coordinate system such that this component is always the  $z$  component. This property will be important later when we consider the intrinsic OAM of the unit cell of a periodic light beam.

The work described here is guided by the aim to blur the distinction between OAM and spin of light by introducing light beams without spin (i.e. linearly polarised light beams) that rotate about more than one point. To this end we investigate the OAM of rectangular lattices of optical vortices [6, 7, 8, 9]. Notably, the rotation can only be about discrete points (the centres of the optical vortices – see Fig. 2), but these can be very densely packed, limited only by fundamental considerations [9, 10]. Such lattices are currently receiving an increasing amount of interest, for example by serving as “conveyor belts” for microscopic particles [11]. We find that the OAM of these lattices has surprising properties.

Throughout this paper we will discuss fields which are strictly periodic; not only the intensity is periodic, but also the phase. The topological charge of each unit cell of such a function is always zero. This vanishing topological charge per unit cell implies that it is not possible to create a strictly periodic array of optical vortices of the same, non-zero, charge [12] without introducing other types of discontinuities that balance the topological charge of the vortices. The tiling discussed in ref. [7], for example, results in discontinuities along the tile edges.

We note that light beams with periodic patterns imprinted in their transverse profile can be generated in a number of ways, for example by interference, through interaction with spatial

light modulators or periodic media (photonic crystals), or in homogeneous devices as result of modulation instabilities. The class of light patterns considered here is characterized by the presence of phase singularities (vortex arrays). The interest in arrays of vortices extends far beyond optics: highly ordered vortex lattices have for instance been observed in rotating Bose-Einstein condensates [13] and in superfluids [14], and they play an important role in fluid dynamics [15, 16].

We have organised this paper as follows. In section 2 we use an example to illustrate our main findings, specifically the seemingly paradoxical dependence on the choice of unit cell. We will resolve this apparent paradox in sections 3 to 5. In section 3 we calculate the angular momentum per unit cell of a general periodic momentum distribution in a plane. In section 4 we introduce a Fourier-based calculation of the OAM per unit cell, which allows us to discuss other effects related to periodic light beams – most notably the Talbot effect – in the context of OAM. In section 5 we discuss the dependence of the OAM per unit cell on the choice of unit cell in the context of finite-sized arrays, before drawing conclusions.

## 2. Example

Here we choose a specific cross-section through an array of optical vortices – shown in Fig. 2 – and discuss its OAM per unit cell. The polarization-independent complex field is of the form

$$\psi(x, y) = (\sin x + i \sin y) \left( \cos \frac{x}{2} \cos \frac{y}{2} \right)^4. \quad (5)$$

The first factor,  $(\sin x + i \sin y)$ , contains a rectangular array of vortices of alternating charges. The second factor,  $(\cos(x/2) \cos(y/2))^4$ , concentrates the intensity around a rectangular array of vortices with a positive charge, which are positioned where  $\cos(x/2) \cos(y/2) = \pm 1$  by multiplying the complex vortex function by an intensity factor which vanishes at the positions of negative-charge vortices; the exponent determines how strongly the intensity is concentrated. While the intensity factor does not affect the phase of the field and therefore the topological charge, it does alter the OAM density.

The OAM per photon for any unit cell of the vortex array given in Eq. (5) is intrinsic: the transverse momentum in a unit cell is zero, i.e.  $P_x = 0 = P_y$  (see Eq. (7)), and therefore it does not matter with respect to which point a cell's OAM and OAM per photon,  $\Omega$  and  $l$ , are calculated. At the same time, all unit cells shown in Fig. 2 are unit cells of the same array. Therefore, as with other quantities of periodic fields, it appears reasonable to think that the OAM per photon of a unit cell is independent of the choice of unit cell.

Figure 3 shows the OAM per photon per unit cell for all choices of smallest possible square unit cells. Contrary to our naive expectation it is clearly dependent on the choice of unit cell and can even change sign. In sections 3 and 4 we will investigate this finding further.

Our main observation is that the angular momentum per unit cell depends on the choice of unit cell. As the angular momentum of an array is the product of the (intrinsic) angular momentum per unit cell and the number of unit cells that make up the array, does this imply that the angular momentum of a periodic light beam also depends on the choice of unit cell? We will discuss this question in section 5.

## 3. Angular momentum of a periodic momentum distribution

We now consider a wave with a periodic transverse profile

$$\psi(x + nX, y + mY) = \psi(x, y), \quad (6)$$

where  $n, m = 0, \pm 1, \pm 2, \dots$  and  $X$  and  $Y$  are the respective lattice periods in the  $x$  and  $y$  directions. From Eq. (1) it follows that the momentum density  $\mathbf{p}_\perp(x, y)$  is also a periodic function. In

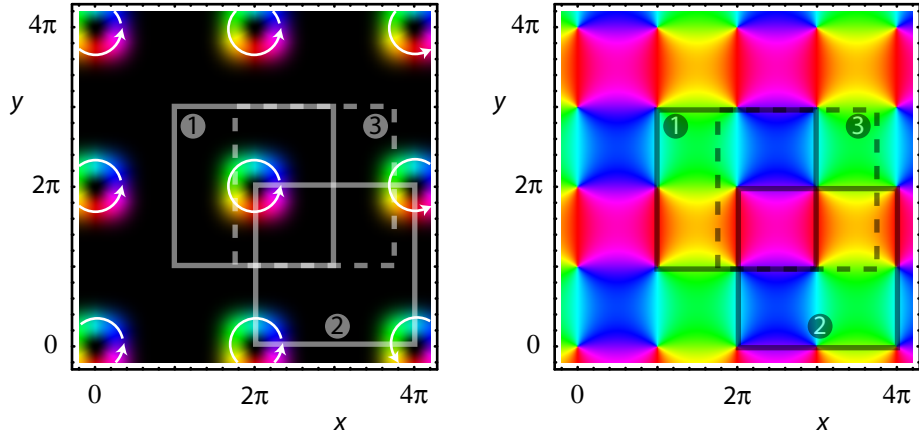


Fig. 2. Example of the field  $\psi(x,y)$  of a rectangular vortex array. The graph on the left shows the intensity cross-section, coloured according to its phase (using the phase-to-colour mapping described in Fig. 1); the graph on the right shows the phase cross-section. Neighbouring vortices have charges with alternating signs (see phase plot); the intensity is concentrated around the vortices with a positive charge. In the left graph, red arrows indicate the transverse momentum density in the beam, which corresponds to a rotation about the vortex centres. This can be clearly seen in the movie (200 KB) showing the time evolution of the phase-coloured intensity distribution, which is contained in the additional multimedia material. The function  $\psi(x,y)$  was calculated using Eq. (5). Specific unit cells that serve as examples throughout this paper are indicated as squares marked '1' to '3'.

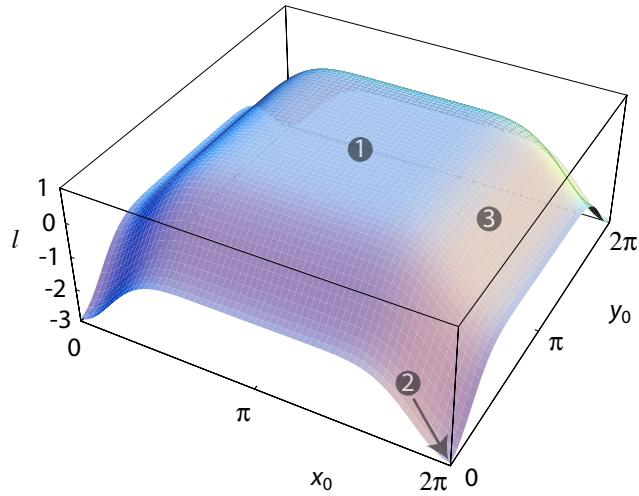


Fig. 3. OAM per photon in units of  $\hbar$ ,  $l$ , of different unit cells of the vortex array shown in Fig. 2. Each unit cell is a square of side length  $2\pi$  with its lower left corner positioned at coordinates  $(x_0, y_0)$ . The values of  $l$  range from approximately  $-2.93$  (in the corners) to  $0.96$  (in the centre). The points corresponding to the sample unit cells highlighted in Fig. 2 are marked '1' to '3'.

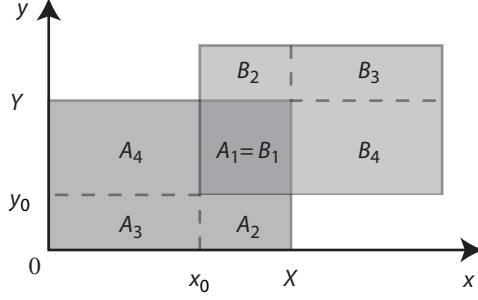


Fig. 4. Unit cells  $A = A_1 + A_2 + A_3 + A_4$  and  $B = B_1 + B_2 + B_3 + B_4$ .

fact, the calculation in this section is applicable to any rectangularly periodic momentum distribution, for example those due to circular polarization in light beams and to arrays of rotating liquids or solids.

Due to the symmetry of the wave given in Eq. (6), it is natural to characterise its properties in terms of rectangular unit cells of the lattice with sides  $X$  and  $Y$ . We restrict ourselves to the case of light fields in which the transverse linear momentum in any unit cell  $D$  vanishes, that is

$$\mathbf{P}_\perp = (P_x, P_y) = \int_D \mathbf{p}_\perp dx dy = 0, \quad (7)$$

where  $\mathbf{p}_\perp = (p_x, p_y)$ . Then  $\Omega_D$ , the OAM in  $D$  according to Eq. (3), is intrinsic [4, 3]. This means that changing the  $(x, y)$  position of the OAM-calculation axis from  $(0, 0)$ , which was implicitly used in Eq. (2), to arbitrary coordinates  $(R_x, R_y)$  results in the same angular momentum:

$$\int_D ((\mathbf{r} - \mathbf{R}) \times \mathbf{p}_\perp)_z dx dy = \int_D (\mathbf{r} \times \mathbf{p}_\perp)_z dx dy. \quad (8)$$

For simplicity we will now consider two rectangular unit cells  $A$  and  $B$  with side lengths  $X$  and  $Y$  whose lower left corners are positioned respectively at the origin and at  $(x_0, y_0)$ , as shown in Fig. 4. Note that it is natural in this context to characterize a unit cell in terms of the coordinates of one of its corners, whereas in the context of section 4 it is conventional to characterize a cell in terms of its center coordinates. We already observed in section 2 that the angular momenta

$$\Omega_A = \int_0^Y \int_0^X (\mathbf{r} \times \mathbf{p}_\perp)_z dx dy \quad (9)$$

and

$$\Omega_B = \int_{y_0}^{y_0+Y} \int_{x_0}^{x_0+X} (\mathbf{r} \times \mathbf{p}_\perp)_z dx dy \quad (10)$$

are not necessarily the same. Clearly the difference is due to the lack of periodicity of the function  $\mathbf{r}$ . In spite of the fact that the angular momentum carried by any cell is independent on the axis position (and indeed on any change  $\mathbf{r} \rightarrow \mathbf{r} + \mathbf{R}$ ) the dependence of the density  $\omega$  on  $\mathbf{r}$  leads to differences between  $\Omega_A$  and  $\Omega_B$ . In the following we analytically evaluate the difference in angular momentum carried by two such unit cells at arbitrary positions.

First of all we observe that any two unit cells “of the same type”, i.e. unit cells whose positions respectively differ by integer multiples of the periods  $X$  and  $Y$  in the  $x$  and  $y$  direction, have the same angular momentum. This is simply due to the periodicity of the linear momentum density and the intrinsic character of the angular momentum carried by a cell. Without loss

of generality we can therefore restrict ourselves to overlapping unit cells  $A$  and  $B$ , as shown in Fig. 4.

We now define  $A_i$  and  $B_i$  ( $i = 1, \dots, 4$ ) as the rectangular parts that respectively add up to  $A$  and  $B$  as shown in Fig. 4. Periodicity guarantees that the momentum distribution in the cell  $B_i$  is the same as inside the corresponding cell  $A_i$ , for any  $i$ . It follows that

$$\begin{aligned}\Omega_B &= \Omega_A + X \int_{A_3+A_4} p_y \, dx \, dy - Y \int_{A_2+A_3} p_x \, dx \, dy \\ &= \Omega_A + X \int_0^{x_0} \int_0^Y p_y \, dy \, dx - Y \int_0^{y_0} \int_0^X p_x \, dx \, dy.\end{aligned}\quad (11)$$

Equation (11) is the main result of this section.

We now apply Eq. (11) to find which distributions  $\mathbf{p}_\perp$  give the same angular momentum  $\Omega$  in *any* cell. It is clear that Eq. (11) is independent of the choice of  $x_0$  and  $y_0$  if and only if

$$\int_0^Y p_y \, dy = 0 \quad (12)$$

for all  $x$  and

$$\int_0^X p_x \, dx = 0 \quad (13)$$

for all  $y$ . As

$$\Omega_A = \int_0^Y \int_0^X x p_y - y p_x \, dx \, dy = \int_0^X x \left( \int_0^Y p_y \, dy \right) dx - \int_0^Y y \left( \int_0^X p_x \, dx \right) dy, \quad (14)$$

equations (12) and (13) imply that  $\Omega_A = 0$ . Therefore the angular momentum carried by a unit cell is independent of the cell's position if and only if the angular momentum for all cell positions is zero. As this is clearly not the case for the vortex-array example in section 2, its orbital angular momentum depends on the choice of unit cell.

We conclude this section by deriving another general property of vortex arrays. Let us consider the integral of the angular momentum over different cell positions,

$$\int_0^X \int_0^Y \Omega_{(x_0, y_0)} \, dx_0 \, dy_0, \quad (15)$$

where  $(x_0, y_0)$  is the position of the lower left corner of the cell. It is easily found that

$$\int_0^X \int_0^Y \Omega_{(x_0, y_0)} \, dx_0 \, dy_0 = 2 \int_0^X \int_0^Y (x_0 P_y - y_0 P_x) \, dx_0 \, dy_0, \quad (16)$$

where  $(P_x, P_y)$  is the total transverse momentum introduced in Eq. (7). As we are considering arrays with intrinsic angular momentum, Eq. (7) implies that

$$\int_0^X \int_0^Y \Omega_{(x_0, y_0)} \, dx_0 \, dy_0 = 0. \quad (17)$$

This result allows to make general predictions about the sign of the angular momentum carried by different cells of an array of vortices. In fact, as the integral (17) over different cell positions vanishes, it follows that if a cell in the array carries a *positive* angular momentum, there is a shifted cell carrying a *negative* angular momentum. Clearly, when we consider continuous spatial arrays, there is also a cell position giving vanishing angular momentum. An illustrative example of this general result is given in Fig. 5.

We note that in this section we did not assume paraxial fields or any light-specific properties, such as Eq. (1), so our results are valid for any type of angular momentum – OAM and spin – of any beam with a rectangular periodicity in the cross section of its phase, intensity and polarization (e.g. [17]).

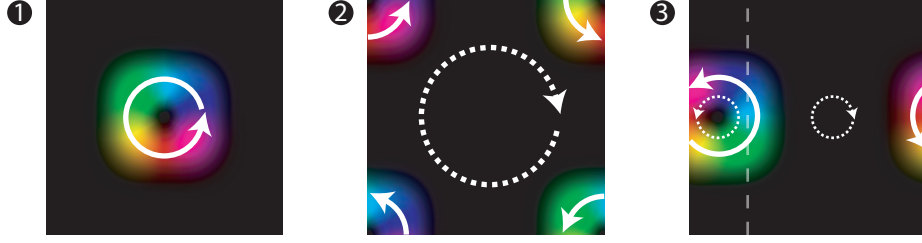


Fig. 5. Schematic of the transverse momentum density in different unit cells of the array shown in Fig. 2. Solid arrows indicate the momentum density in the beam. Comparison of cells ‘1’ and ‘2’ shows that in different unit cells the bulk of the momentum density can be at different radii from the cell’s centre (as the OAM in each unit cell is intrinsic and therefore independent of the axis position, we might as well calculate it with respect to a symmetric choice of axis position, namely the centre of the unit cell), leading to a larger OAM density according to Eq. (2), and that the circulation of the momentum density with respect to the axis (dotted arrow in ‘2’) can even be reversed, resulting in OAM of the opposite sign. The respective OAM per photon in unit cells ‘1’ and ‘2’ is  $0.96\hbar$  and  $-2.93\hbar$ . In cell ‘3’ the OAM in each of the two parts of the cell (separated by the dotted white line) is intrinsic and equal and opposite that in the other part (the circulation of the momentum density in opposite directions is again indicated by dotted arrows), so the OAM in the whole cell is 0.

#### 4. OAM of periodic light beams on propagation

Light beams that are periodic in the  $x$  and  $y$  direction can also be periodic in the  $z$  direction – the Talbot effect [18]. It is therefore natural to investigate the OAM contained in the (three-dimensional) unit cells of such a beam.

Mathematically, our periodic optical fields are naturally described as Fourier series in  $x$  and  $y$ . Not only does this enable an alternative proof for the disappearance of the average OAM over choice of cell positions, but it allows the investigation of the OAM on propagation of the beams in the  $z$  direction.

Any beam with rectangular lattice periodic symmetry in the transverse plane can be written as a Fourier series

$$\psi(x, y) = \sum_{m, n} a_{m, n} \exp(2\pi i(mx/X + ny/Y)), \quad (18)$$

where the sum in  $m, n$  is over all integers (positive and negative), the  $a_{m, n}$  are complex coefficients, and all sums are assumed to converge.

It is straightforward to compute all quantities explicitly (such as  $\nabla\psi, \mathbf{p}$ , etc.) for  $\psi(x, y)$  in the form (18). Substitution into equations (1) and (2) gives the  $z$ -component of the OAM density:

$$\omega(x, y) = 2\pi \operatorname{Re} \sum_{m, m', n, n'} a_{m', n'}^* a_{m, n} \left( \frac{nx}{Y} - \frac{my}{X} \right) \exp \left( 2\pi i \left( \frac{(m - m')x}{X} + \frac{(n - n')y}{Y} \right) \right). \quad (19)$$

The total transverse linear momentum  $\mathbf{P}_\perp$ , which vanishes when the angular momentum is intrinsic (see Eq. (8)), is

$$\mathbf{P}_\perp = 2\pi \sum_{m, n} (mY, nX) |a_{m, n}|^2. \quad (20)$$

For the present purposes, it is convenient to describe the position of a unit cell in terms of its

centre  $(x_c, y_c)$ . The  $(x_c, y_c)$ -dependent total OAM in the unit cell is easily calculated to be

$$\begin{aligned}
\Omega_{(x_c, y_c)} &= \int_{y_c-Y/2}^{y_c+Y/2} \int_{x_c-X/2}^{x_c+X/2} \omega(x, y) dx dy \\
&= \mathbf{r}_c \times \mathbf{P}_\perp \\
&\quad + \text{Im} \sum_{m, n} a_{m, n} \left( nX^2 \sum_{m' \neq m} a_{m', n}^* (-1)^{m-m'} \frac{\exp(2\pi i(m-m')x_c/X)}{m-m'} \right. \\
&\quad \left. - mY^2 \sum_{n' \neq n} a_{m, n'}^* (-1)^{n-n'} \frac{\exp(2\pi i(n-n')y_c/Y)}{n-n'} \right). \tag{21}
\end{aligned}$$

This is the general expression for the OAM in a unit cell of a periodic beam.

When the OAM is intrinsic,  $\mathbf{P}_\perp$  is zero and the first term in (21) vanishes. In that case, there is no constant term in the right-hand side of Eq. (21), which is a Fourier series, so the average of  $\Omega_{(x_c, y_c)}$  over all cell positions is zero (as expected – see Eq. (17)).

We now want to investigate the behaviour of the OAM in a unit cell on propagation of the light field. We perform the calculation for monochromatic light fields. To be able to evaluate a light field  $\psi$  in other planes, we substitute for the expression for each Fourier component in the  $z = 0$  plane the expression that explicitly takes its  $z$  dependence into account:

$$\exp(i(k_x x + k_y y)) \rightarrow \exp(i(k_x x + k_y y + k_z z)), \tag{22}$$

where  $k_x = 2\pi m/X$  and  $k_y = 2\pi n/Y$  are the transverse wave numbers. For  $k_z$  we use the approximation

$$k_z = (k^2 - k_x^2 - k_y^2)^{1/2} \approx k - (k_x^2 + k_y^2)/(2k), \tag{23}$$

which is valid for paraxial beams, i.e. beams that only contain Fourier-components with small values of  $m$  and  $n$ . The wave  $\psi$  can then be calculated at all points in space:

$$\psi_{\text{prop}}(x, y, z) = \sum_{m, n} a_{m, n} \exp(2\pi i(mx/X + ny/Y - (m^2/X^2 + n^2/Y^2)\pi z/k)). \tag{24}$$

Alternatively, Eq. (24) can be derived from the paraxial wave equation [19]. We ignore here phase term  $\exp(ikz)$  as it affects only the phase of the whole beam. Specifically it does not affect the transverse momentum and the angular momentum in the  $z$  direction.

If the transverse periodicities are rationally related, i.e. if coprime positive integers  $M, N$  exist such that  $MX = NY = Z$  for some length  $Z$ , then (24) becomes

$$\psi_{\text{prop}}(x, y, z) = \sum_{m, n} a_{m, n} \exp(2\pi i(mx/X + ny/Y - (m^2 M^2 + n^2 N^2)(\pi/kZ^2)z)). \tag{25}$$

i.e. the beam is periodic in  $z$ , ‘reviving’ at the Talbot distance  $\tau = Z^2 k/\pi$  [18].

Paraxial propagation, and specifically Talbot periodicity, can be built into the earlier equations by replacing the Fourier coefficients as follows:

$$a_{m, n} \rightarrow a_{m, n} \exp(-2\pi i(M^2 m^2 + N^2 n^2)z/\tau). \tag{26}$$

The total angular momentum per unit cell  $\Omega_{(x_c, y_c)}$  is now a (periodic) function of  $z$  whose average over  $z$  does not necessarily vanish.

As an example we consider the beam (5) of section 2. Evidently it has a finite Fourier series representation and square symmetry ( $X = Y = 2\pi$ ), which simplifies the calculation. Figure 6 shows the beam’s intensity cross section for different values of the propagation distance  $z$  and

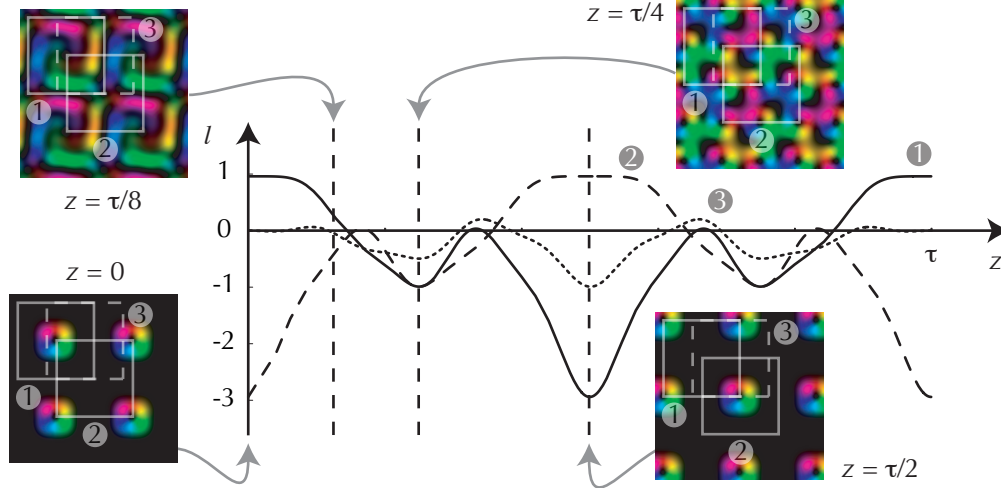


Fig. 6. OAM per photon in units of  $\hbar$ ,  $l$ , per unit cell on propagation through one Talbot period,  $\tau$ , calculated for the unit cells highlighted in Fig. 2 of the beam given at  $z = 0$  by Eq. (5). The curves corresponding to cells '1', '2' and '3' are respectively drawn solid, dashed and dotted. Insets show the intensity cross-sections across the beam at  $z = 0$ ,  $\tau/8$ ,  $\tau/4$  and  $\tau/2$ ; the position of the unit cells is marked. The additional multimedia material contains a movie (268 KB) showing the evolution of the beam cross-section in unit cell '1' over one Talbot period.

the OAM per photon for different unit cells as a function of  $z$ . It can be seen that propagation through half a Talbot period ( $z = \tau/2$ ) shifts this beam, indeed any beam for which both  $M$  and  $N$  are odd, through half a transverse period in the  $x$  and  $y$  direction, i.e.

$$\Psi_{\text{prop}}(x, y, z + \tau/2) = \Psi_{\text{prop}}(x \pm X/2, y \pm Y/2, z). \quad (27)$$

Therefore the cell-averaged OAM per photon in unit cell '1' is the same as that in cell '2' half a Talbot period later.

The average of  $\Omega_{(x_c, y_c)}(z)$  over a Talbot distance is not necessarily 0, but given for any arbitrary beam by

$$\langle \Omega_{(x_c, y_c)} \rangle_z = \frac{1}{2} \text{Im} \sum_{m, n \neq 0} a_{m, n} \left( a_{-m, n}^* \frac{n}{m} X^2 \exp(4\pi i m x_c / X) - a_{m, -n}^* \frac{m}{n} Y^2 \exp(4\pi i n y_c / Y) \right). \quad (28)$$

Inspection reveals that the average of  $\Omega_{(x_c, y_c)}$  over its propagation period is doubly periodic in  $x_c$  and  $y_c$ , as Eq. (27) would suggest. As before, the average over the transverse position  $(x_c, y_c)$  vanishes as this Fourier series has no constant term.

## 5. Finite arrays and edge effects

In section 2 we ask whether the angular momentum of a periodic light beam – which is the product of the cell-choice-dependent angular momentum per unit cell and the number of unit cells that make up the light beam – also depends on the choice of unit cell. It follows from our result that in a truly periodic – and therefore necessarily infinite – light beam the angular momentum carried by a transverse slice of the beam is not well-defined.

Any real-life periodic light beam has a *finite* size and therefore can only consist of a finite number of unit cells. Figure 7 shows an example of a finite vortex-array: a circular section of

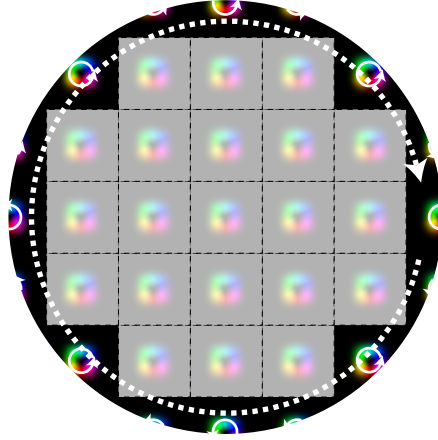


Fig. 7. Finite-size optical-vortex array. The centre of the array is covered by unit cells (shown with reduced contrast). An area at the edge of the beam (full contrast) cannot be covered by whole unit cells. The momentum density in the edge is indicated by white arrows; solid arrows indicate the actual momentum density, the dashed arrow indicated the “trend”.

the example shown in Eq. (5). It is clear that for any particular choice of unit cell only part of the beam that can be covered by complete unit cells; an area near the edge of the beam remains uncovered. The angular momentum in the whole beam is the sum of the angular momenta contained in the part of the beam that is covered by the unit cells, which is simply the angular momentum per unit cell times the number of unit cells, and that in the edge of the beam. The shape of the edge part changes depending on the choice of unit cell; the angular momentum contained in it is always the difference between the angular momentum in the whole beam and that contained in the part covered by unit cells.

That the outer regions of light beams can contain large amounts of OAM has been observed previously (e.g. [20]). However, often when integrating a quantity over a finite area (or volume), the contribution of the edge becomes insignificant as the area becomes larger. The following handwaving argument illustrates why this is not the case for angular momentum. Consider a circular light beam of radius  $r$ . We assume that the edge area is on average of a width that is independent of  $r$  and that the average momentum density is also constant. The edge area is then approximately the average width times the circumference of the beam, so it is approximately proportional to  $r$ . The angular momentum density near the edge, calculated with respect to the centre of the beam, is proportional to the momentum density and  $r$ . This implies that the angular momentum in the edge is proportional to  $r^2$ . The number of unit cells covering the centre of the beam also goes approximately with  $r^2$ , so we conclude that the angular momentum in the edge remains significant compared to that in the main part of the beam, even for large beams.

## 6. Conclusions and ideas for generalizations

This work was motivated by the desire to create orbital angular momentum that is spin-like in a number of ways. Here we specifically wanted to create light beams whose orbital angular momentum, when absorbed over a large enough area, was non-zero and approximately proportional to the area. From the results presented in this paper we conclude that this is not possible with strictly rectangularly periodic light beams.

The most likely candidate for such a light beam would appear to be an array of optical

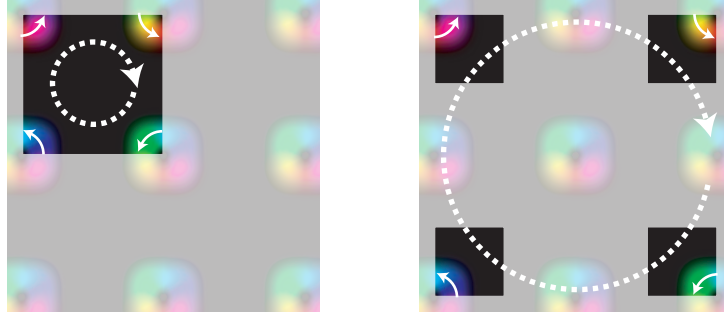


Fig. 8. Example of the dependence of the OAM per photon in a unit cell on its shape. The OAM per photon in the unit cell on the left is  $-2.94\hbar$ , that in the unit cell on the right is  $-6.84\hbar$  (note that the four parts of the unit cell are not connected). The actual unit cell is shown in full contrast; some of the surrounding beam is also shown, in reduced contrast. Like in Fig. 5, the larger OAM per photon in the cell on the right is again due to the fact that the bulk of the momentum density is at a larger radius from the cell's centre.

vortices with an intrinsic OAM per unit cell. Because of the periodicity of the transverse profile of the beam we would have expected a variation of the OAM that depends on the exact details of the absorbing area; for an absorbing area that is a unit cell of the array we would have expected, somewhat naively, a position-independent value of the OAM. What we found to our surprise is that the OAM in a unit cell not only depends on the position, but it depends on the position so strongly that it is always possible to find a position for which the OAM changes sign. The angular momentum of part of any momentum distribution with intrinsic angular momentum is independent of the position of that part only if the angular momentum is zero.

It would be interesting to generalize our results to other array symmetries and to investigate in detail the dependence of the OAM per photon per unit cell as a function of the shape of the unit cell. Figure 8 shows an example of two unit cells with different shapes: the square unit cell with the greatest modulus of the OAM per photon ( $-2.94\hbar$ ), and a unit cell with a non-square shape (in fact a non-connected shape) with a modulus of the OAM per photon that is significantly higher ( $-6.84\hbar$ ). The latter cell is constructed by splitting up a square unit cell into four parts and moving those by integer multiples of the lattice periods. In fact, by increasing the separation of the parts the OAM per photon in the unit cell can be made arbitrarily high.

Finally, we note that the dependence on the choice of unit cell is not peculiar to vortex arrays, optical or otherwise, but applies to any rectangularly periodic momentum distribution.

### Acknowledgements

Many thanks to Michael Berry, Stephen Barnett, Erika Andersson, Gian-Luca Oppo, L. Allen, Gavin Sinclair, Jonathan Leach and Miles Padgett for useful discussions. Part of this work was performed while Mikhail Vasnetsov was an EPSRC *Visiting Fellow* at the University of Glasgow (grant no. EP/B000028/1). Roberta Zambrini is supported by EPSRC (grant no. SO3898/01). Johannes Courtial and Mark Dennis are Royal Society University Research Fellows.